Check for updates

Treatment planning of intracranial lesions with VHEE: comparing conventional and FLASH irradiation potential with state-of-the-art photon and proton radiotherapy

A. Muscato[1,2,3], L. Arsini[2,4], G. Battistoni[5], L. Campana[1], D. Carlotti[4,6], F. De Felice[7], A. De Gregorio[4,2]*, M. De Simoni[2,8], C. Di Felice[9], Y. Dong[5], G. Franciosini[1,2], M. Marafini[2,3], I. Mattei[5], R. Mirabelli[1,2], S. Muraro[5], M. Pacilio[9], L. Palumbo[1,2], V. Patera[1,2], A. Schiavi[1,2], A. Sciubba[1,10], M. Schwarz[11], S. Sorbino[1], V. Tombolini[7], M. Toppi[1,2], G. Traini[2], A. Trigilio[4,10] and A. Sarti[1,2]

[1]Dipartimento di Scienze di Base e Applicate per l'Ingegneria, Sapienza Università di Roma, Roma, Italy, [2]INFN Sezione di Roma I, Roma, Italy, [3]Museo Storico della Fisica e Centro Studi e Ricerche Enrico Fermi (CREF), Roma, Italy, [4]Dipartimento di Fisica, Sapienza Università di Roma, Roma, Italy, [5]INFN Sezione di Milano, Milano, Italy, [6]Radiation Oncology, Fondazione Policlinico Universitario Campus Bio-medico, Rome, Italy, [7]Dipartimento di Scienze Radiologiche, Oncologiche e Anatomo Patologiche, Sapienza Università di Roma, Roma, Italy, [8]Departement of Medical Physics Ludwig Maximilians Universität München (LMU) Munich, Munich, Germany, [9]Unità di Fisica Sanitaria, Azienda Ospedaliero-Universitaria Policlinico Umberto I, Roma, Italy, [10]Istituto Nazionale di Fisica Nucleare (INFN) Sezione dei Laboratori di Frascati, Roma, Italy, [11]Radiation Oncology Department, University of Washington & Fred Hutchinson Cancer Center, Seattle, CA, United States

The treatment of deep-seated tumours with electrons of very high energies (VHEE, 70−150 MeV) has already been explored in the past, suggesting that a dosimetric coverage comparable with state-of-the-art proton (PT) or photon radiotherapy (RT) could be achieved with a large (> 10) number of fields and high electron energy. The technical and economical challenges posed by the deployment of such beams in treatment centres, together with the expected small therapeutic gain, prevented the development of such technique. This scenario could radically change in the light of recent developments that occurred in the compact, high-gradient, electron acceleration technology and, additionally, of the experimental evidence of the sparing of organs at risk achieved in ultra-high dose rate irradiation, also referred to as FLASH. Electrons with the energy required to treat intracranial lesions could be provided, at dose rates compatible with what is needed to trigger the FLASH effect, by accelerators that are a few metres long, and the organ sparing could be exploited to significantly simplify the irradiation geometry, decreasing the number of fields needed to treat a patient. In this paper, the case of two patients affected by a chordoma and a meningioma, respectively, treated with protons in Trento (IT) is presented. The proton plans have been compared with VHEE plans and X-ray intensity-modulated radiotherapy (IMRT) plans. The VHEE plans were first evaluated in terms of physical dose distribution and then assuming that the FLASH regimen can be achieved. VHEE beams demonstrated their potential in obtaining plans that

have comparable tumour coverage and organs at risk sparing when benchmarked against current state-of-the-art IMRT and PT. These results were obtained with a number of explored fields that was in the range between 3 and 7, consistent with what is routinely performed in IMRT and PT conventional irradiations. The FLASH regimen, in all cases, showed its potential in reducing damage to the organs placed nearby the target volume, allowing, particularly in the chordoma case where the irradiation geometry is more challenging, a better tumour coverage with respect to the conventional treatments.

1 Introduction

In the framework of constant research and effort to improve the therapeutic efficacy of deep-seated tumour treatments with external beam radiotherapy (EBRT), different radiation types have been explored in the past. However, the vast majority of treatments are delivered using X-ray radiotherapy, and a smaller fraction of patients is treated with particle therapy (PT) delivered with either protons or heavier ions.

The experience gained so far allowed both IMRT and PT to obtain remarkable results, providing a high level of dose conformity to the target volume. As the therapeutic window of IMRT also depends on normal tissue complication probability, a continuous effort is devoted to improve the sparing of the organs at risk (OARs). In this respect, IMRT and PT treatments have different characteristics and have to be carefully optimised in different ways, providing optimal solutions to different disease sites on the specific position and accessibility of the target volume. As electrons are light-charged particles, their unique features of interaction with matter could be additionally exploited to provide treatments capable of overcoming limitations of IMRT and PT in specific districts or irradiation modalities.

Electrons with energies in the range of 60–120 MeV (VHEE) can be used to treat deep-seated tumours, as they are capable of reaching the needed depth and exhibiting a wide dose peak, whose position changes according to the beam energy. Their use have already been explored in the past [1–3], and a performance comparable with volumetric modulated arc therapy (VMAT) and proton irradiations was demonstrated, at the cost of using a complex irradiation system with many fields (13 or more) or high beam energy (at least 100 MeV) [4, 5]. At the same time, the production of high-energy beams required long accelerating sections that were not easily compatible with existing clinical centres. These conditions contributed, in the past, to make the VHEE solution less cost-effective for a clinical centre with respect to IMRT or other photon-based modalities.

Nowadays, the creation of an accelerating, compact, lower-cost structure for producing high-energy electron fields is possible with the advent of C-band accelerating structures, which is capable of accelerating electrons with the required high charge and fields of up to 50 MeV/m in the hospital setting [6].

In addition, there is increasing evidence from preclinical studies showing that if the dose rate is radically increased (~40 Gy/s, at least) with respect to conventional treatments (~0.01 Gy/s), induced radiotoxicity in healthy tissues can be significantly reduced, while maintaining the same cytotoxic effects on cancer cells. Such effects will be further referred to as the FLASH effect [4, 7–9]. The implementation of FLASH beams in clinical centres [10] still has to overcome significant technical challenges. Although FLASH intensities have already been achieved for proton and electron beams (e.g., the low-energy electron beams used for intra-operative radiation therapy), mostly in pre-clinical settings, the implementation of FLASH IMRT with photons is still in its early development stage [8, 11].

The recent advancements in electron accelerating technology, together with the experimental exploration of the FLASH effect, have re-fuelled the interest in the planning and delivery of VHEE for therapeutic applications [12].

In this manuscript, following the approach previously described in [13], the potential of VHEE, with a low number of fields and maximal energy of 130 MeV to treat intracranial lesions, has been studied. The results of conventional irradiation have been compared with state-of-the-art IMRT and PT treatments, and, in addition, the FLASH effect potential for the treatment of such pathologies has been explored.

The first study to explore the feasibility of VHEE to treat deep-seated tumours with a limited number of irradiation fields ([13]) was made on a prostate cancer case, performing comparisons with high-quality results that can be attainable with IMRT and PT at conventional dose rates. In this work, a meningioma and a chordoma case were chosen to investigate how VHEE could be exploited to handle challenging treatments, where the planning target volume (PTV) is closely surrounded by several OARs whose sparing is made difficult by the patient's anatomy and the corresponding dosimetric prescriptions and constraints. In addition, the reason for choosing this region and, in particular, intracranial lesions to assess the FLASH potential is that they are an excellent ground to test the potential of conventional and FLASH irradiation in providing additional sparing to the OARs that are currently limiting the dose prescription to PTV.

The selected cases, dose prescriptions, dosimetric constraints for the OARs, and the treatment plans optimised at the Trento PT Centre (Azienda Provinciale per i Servizi Sanitari, APSS—Trento[1]) are documented. Details are also provided based on the plans

---

1 https://www.apss.tn.it/

TABLE 1 Planning prescriptions for patient M1. D_{max} and D_{mean} are the maximum and average dose absorbed in the volume of interest, respectively. V_{XX} is the fractional volume of a given OAR (or PTV) receiving a minimum dose of (XX Gy). $V_{95\%} > 95\%$ requirement means that 95% of the volume should receive more than 95% of the prescribed dose. $D_1 \leq YY$ Gy requirement means that the minimum dose in the hottest 1% of the volume should not exceed YY Gy. Total volume (in cc) of the PTV and OARs is listed in the last column.

Patient M1	Dosimetric constraint	Volume (cc)
PTV	$V_{95\%} > 95\%$, $D_{max} \leq 105\%$	20.71
Optic nerves	$D_1 \leq 54$ Gy (RBE)	0.95
Chiasm	$D_1 \leq 54$ Gy (RBE)	0.03
Posterior optical path	$D_1 \leq 54$ Gy (RBE)	0.45
Eyeballs	$D_1 \leq 40$ Gy (RBE)	8.14
Brainstem	$D_1 \leq 54$ Gy (RBE)	28.19
Carotid arteries	$D_{max} \leq 105\%$	1.15

TABLE 2 Planning prescriptions for patient C1. D_{max}, D_{mean}, V_{XX}, and D_1 definitions and uses are same as those explained in the caption of Table 1.

Patient C1	Dosimetric constraint	Volume (cc)
PTV	$V_{95\%} > 95\%$, $D_{max} \leq 107\%$	99.15
PTV boost	$V_{95\%} > 95\%$, $D_{max} \leq 107\%$	71.94
Brainstem	$D_1 \leq 55$ Gy (RBE)	27.09
Spinal cord	$D_1 \leq 54$ Gy (RBE)	8.25
Parotid glands	$D_{mean} \leq 26$ Gy(RBE)	26.26
Middle ears	$D_{mean} \leq 30$ Gy(RBE)	3.80
Cochlea	$D_{mean} \leq 35$ Gy(RBE)	0.35

optimised in conventional irradiation modality for both IMRT and VHEE. The field's characteristic definition and the process of VHEE pencil beam fluence optimisation have also been detailed. The comparison of actual delivered plans (protons) and IMRT and VHEE plans with and without including the FLASH effect is presented in the Results section followed by a discussion on the implications of the findings in the landscape of VHEE treatments delivered in both conventional and FLASH modalities.

2 Methods

Two patients who underwent PT in Trento (at the APSS centre) to treat a chordoma (hereinafter, patient C1) and a meningioma (M1) were chosen for this study. The patients were treated with protons using a conventional dose rate (~Gy/min), and the prescriptions are currently in use at the Trento therapy centre. The target volumes were identified, and the constraints on PTV coverage, OAR sparing, and details on the irradiation approach were defined. More information about the two PT plans, containing the prescriptions expressed in terms of the biological dose and hence in Gy (RBE) or absorbed dose multiplied by the relative biological effectiveness (RBE), is reported as follows:

- Patient M1: Three fields were used, with a prescription to the PTV of 54 Gy(RBE) in 27 fractions. The dosimetric constraints are listed in Table 1.
- Patient C1: Four fields were used. The treatment was delivered with a simultaneously integrated boost (SIB) technique for a total dose of 60 Gy(RBE) to the boost PTV and 54 Gy(RBE) to the PTV in 30 fractions. A sequential boost of 6 Gy (RBE) in three fractions was then delivered to the boost PTV increasing its final dose to 66 Gy(RBE). The dosimetric constraints are listed in Table 2.

Both treatment plans had to fulfil the planning goals reported in the corresponding table (1 or 2 for M1 and C1, respectively) for the most relevant OARs identified for each treatment.

The clinical proton plans delivered to the patients were sent to the Medical Physics Unit of Policlinico Umberto I in Rome to carry out the IMRT treatment planning, together with the dose prescriptions, the details about the OARs constraints, and the computed tomography (CT) imaging data. The same information was also used to plan VHEE treatments.

The IMRT plans were optimised assuming a static field delivered on a 6 MV-Elekta Versa HD linear accelerator (Elekta [14]). Plans were optimised using the Pinnacle [15] software suite (RTP system version 16, https://pinnacle-software.com/), according to the prescribed dose and constraints provided by the Trento APSS particle therapy centre. Both plans comprised seven fields and matched the requirements set in Table 1 and Table 2.

2.1 VHEE plans

While the IMRT and PT plans can be optimised by means of commercial software used in clinical practice, no medically certified software suite is currently available for the planning of VHEE. In addition, VHEE planning lacks a therapeutic protocol that would be helpful in choosing irradiation geometry. For this reason, plan optimisation software based on the inverse planning approach that uses the absorbed dose relative to pencil beams as an input had to be developed from scratch. The details about the implemented software and the optimisation strategy are discussed in a previous study [13].

When producing the absorbed dose maps needed for the planning procedure, the details of the beam characteristics and the beam acceleration and delivery technology play a crucial role. The specific details (e.g., percentage depth dose distributions and penumbra) of the electron beams considered for the treatment of deep-seated tumours can be found in [16]. There are currently several attempts made at providing the technology needed to provide VHEE, with the required intensity in the treatment room of a therapy centre. First of all, there are radio frequency (RF)-based approaches, like the ones pursued in the Phaser collaboration [5] or the ones exploiting the C-band acceleration technology [6]. A different approach foresees the use of the laser-driven acceleration principle, and it is currently investigated both at the CLEAR facility at CERN [17] and at the Intense Laser Irradiation Laboratory at CNR-INO [18] in Pisa, Italy. In this study, the compact C-band solution detailed in [6], which is suitable to be implemented with a low number of fields and capable of being

TABLE 3 Field electron energies used to perform treatment simulation for the M1 and C1 patients under study. Energies up to 130 MeV were necessary in order to match the electron absorbed dose peak centre with the PTV region.

M1—energy [MeV]						
	Field 1	Field 2	Field 3	Field 4	Field 5	Field 6	Field 7
Three fields	110	110	100	-	-	-	-
Seven fields	90	100	100	110	100	100	90
M1—gantry angle [degrees]						
Three fields	250°	110°	270°	-	-	-	-
Seven fields	80°	110°	140°	180°	220°	250°	280°
C1—energy [MeV]						
Four fields	120	90	90	120	-	-	-
Seven fields	120	80	60	60	60	60	80
C1—gantry angle [degrees]						
Four fields	165°	195°	55°	305°	-	-	-
Seven fields	0°	40°	80°	120°	240°	280°	320°

delivered with an "active scanning"-like approach, was considered and implemented due to its advanced technological readiness level when compared with the laser-plasma-based solutions.

Using the information from the patient planning CT, the entry points, size, and aperture of the electron pencil beams used to irradiate the PTV were defined following an approach similar to active scanning implemented in proton beam delivery. A plane perpendicular to the line joining the electron beam emission point with the PTV centre was used to project the PTV and define the area that has to be covered by the single pencil beam in each field. The overall field geometrical information was inherited from the RT and PT plans used for comparison. For the definition of the number and irradiation geometry of each VHEE pencil beam inside a given field, the only additional input needed was the beam angular divergence. A compact C-band technology was assumed, as in [13], capable of delivering such beams, and hence, an angular aperture of ∼ (O mrad) with a negligible energy spread [6] was used when setting up the beam model for MC simulations.

The FWHM of each pencil beam was set to 1 cm, a reasonable value for electrons of such energy whose target is a deep-seated tumour and hence experience a significant broadening due to multiple scattering interactions. All these parameters are specific of the beam acceleration technique that has been assumed for the delivery of VHEE beams [6] and will have to be updated when exploring other solutions (e.g., VHEE from laser-plasma acceleration).

Once the size and spacing of each pencil beam were defined, their number was computed. Then, using a single pencil beam aiming at the centre of the PTV, the energy needed to place the absorbed dose peak at the centre of the PTV was computed. Two beam configurations were defined for each patient: three or seven fields for M1 and four or seven fields for C1, using the beam directions chosen for IMRT and PT plans. The energies needed to irradiate the two targets are shown in Table 3. In all cases, the energy was less than 150 MeV.

Such evaluations were conducted by means of an accurate FLUKA [19, 20] Monte Carlo (MC) simulation that used, as input, the patient's CT scan. The simulation that allowed us to evaluate the field energy was also used to build the absorbed dose map for each pencil beam of each field and eventually compute the dose maps used as inputs for the pencil beam fluence optimization algorithm.

To reduce the impact of statistical fluctuations on the absorbed dose distribution, each pencil beam simulation was performed using 10^6 events. The robustness of the results was verified by changing the random seeds used for the simulation and obtaining absorbed dose maps that showed negligible discrepancies on the whole CT volume.

The absorbed dose maps, normalised to the number of primaries used in the simulation, for the plans with three and seven fields for patient M1 are shown in Figure 1. No treatment optimisation was performed in this case, i.e., the figures show the absorbed dose for pencil beams that contain 10^6 electrons each which are the inputs for the optimisation step.

2.2 Treatment optimisation

Once the absorbed dose maps have been obtained performing MC simulations for each PB in the treatment plan, the fluence of each PB was optimised to ensure the required PTV coverage and OAR sparing. The implemented algorithms are similar to the previous prostate cancer study ([13]) and are similar to those used in the active scanning TPS used for PT [21]. A cost function with two terms was used: the first term constrains the absorbed dose in the PTV to the target value, while the other term is activated whenever a threshold in the OAR voxels is surpassed. Considering the different priorities when minimising the cost function, a weighing strategy was adopted when including the PTV, OARs, and normal tissue voxels, consistent with what has been carried out in standard software tools used for TPS planning (e.g., Pinnacle). The output of the optimisation process is the absorbed dose map used to
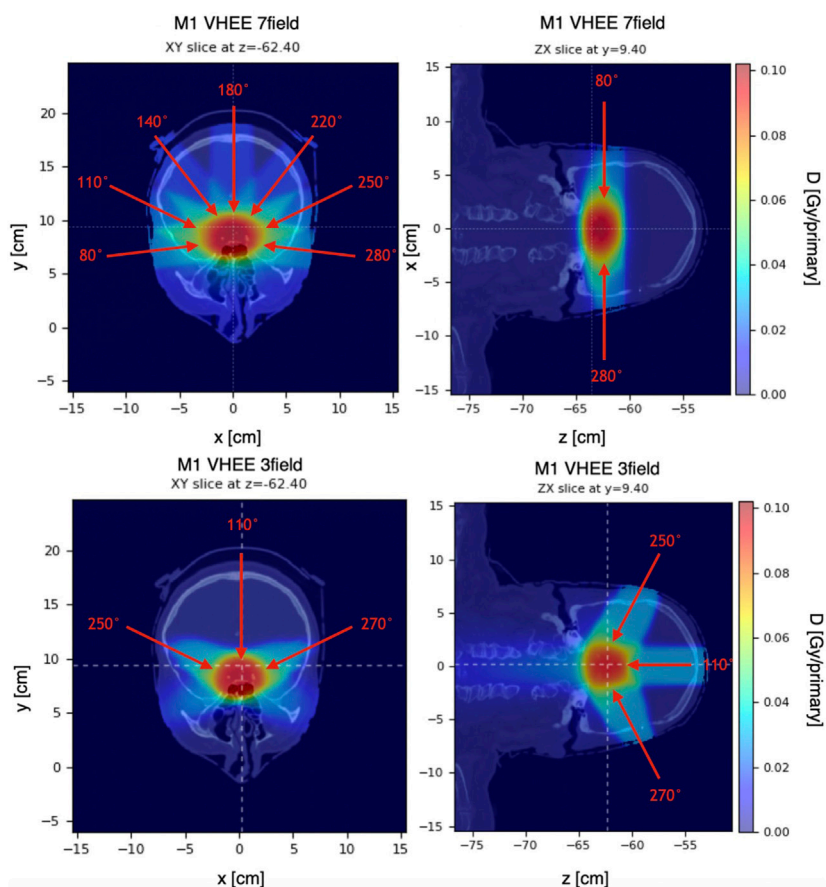
FIGURE 1
Absorbed dose distribution of M1, normalised to the number of primaries, used as an input for the optimisation process. Figures on the left show the configuration using three fields (proton-like), while the figures on the right show the configurations with seven fields (IMRT-like). All pencil beams have 10^6 electrons.

compute dose volume histograms (DVHs) and compare with the standard RT and PT treatments.

The same fractionation scheme (with 2 Gy fractions) implemented in the delivered PT plans was adopted when optimising the IMRT and VHEE plans delivered in the conventional mode.

2.3 FLASH effect modelling

The first aim of our study is to compare absorbed dose distributions from IMRT and PT treatments with VHEE optimised plans, showing the potential of high-energy electrons for treatment planning without any potential gain from the ultra-high dose rate irradiation. Then, the possible impact of the FLASH effect in increasing the treatment efficacy [22, 23] was also studied. Particularly, the study focused on how the reduced damage in the OARs can be exploited to increase the prescription dose of the PTV, allowing for better tumour control. Therefore, the treatment delivery was assumed to satisfy the requirements of the dose rate (DR) that were needed to trigger the FLASH effect in OAR sparing (DR larger than 40 Gy/s).

To quantify the decrease in radiation-induced toxicity in normal tissues due to the FLASH approach, when comparing to conventional radiotherapy, the FLASH modifying factor (FMF)

dependent on the absorbed dose in each voxel was implemented according to [24]. The FMF has been defined as proposed in [24]:

$$FMF = \frac{D_{CONV}}{D_{UHDR}}\bigg|_{Isoeffect,}$$

and the dependence on the absorbed dose (D) was implemented, according to [24], as follows:

$$\text{FMF}(D)_{\text{FMF}^m,D_T} = 1 - \text{FMF}^m \frac{D_T}{D} + \text{FMF}^m \quad \text{for} \quad D > D_T, \quad (1)$$

while it was taken to be equal to 1 for $D \le D_T$.

The parameters D_T and FMF^m that quantify the aforementioned threshold must be carefully selected to determine which significant contributions from the FLASH effect are expected and what is the asymptotic or maximal gain for the sparing of the OARs under study. In this manuscript, the absorbed dose to be used in FMF modelling was assumed to be the total absorbed dose associated with the treatment, whereas the D_T value was fixed to 20 Gy. Such value amounts to nearly one-third of the whole treatment and has been chosen to signify that under real clinical conditions to trigger the FLASH effect, a sizeable dose needs to be absorbed by normal tissues in order to result in an appreciable sparing.
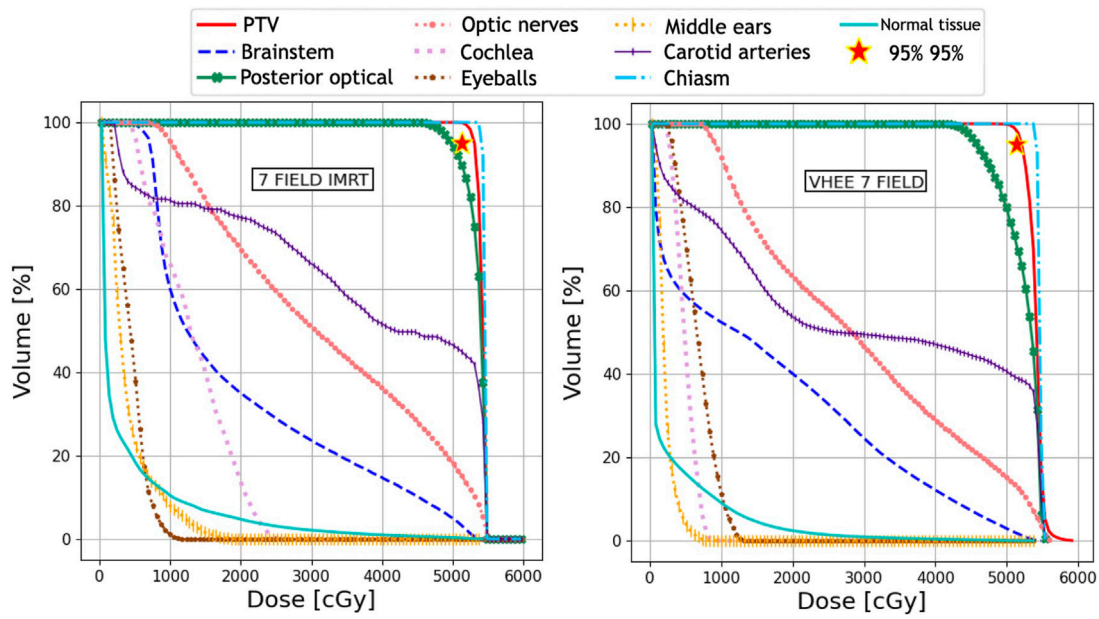
FIGURE 2
Plan comparison between IMRT and VHEE for patient M1. DVHs for the PTV and OARs from the IMRT plan are reported on the left, whereas the VHEE results obtained assuming an irradiation with seven fields are shown on the right. The absorbed dose relative to the unspecified normal tissue (NoT in the legend) is also shown.
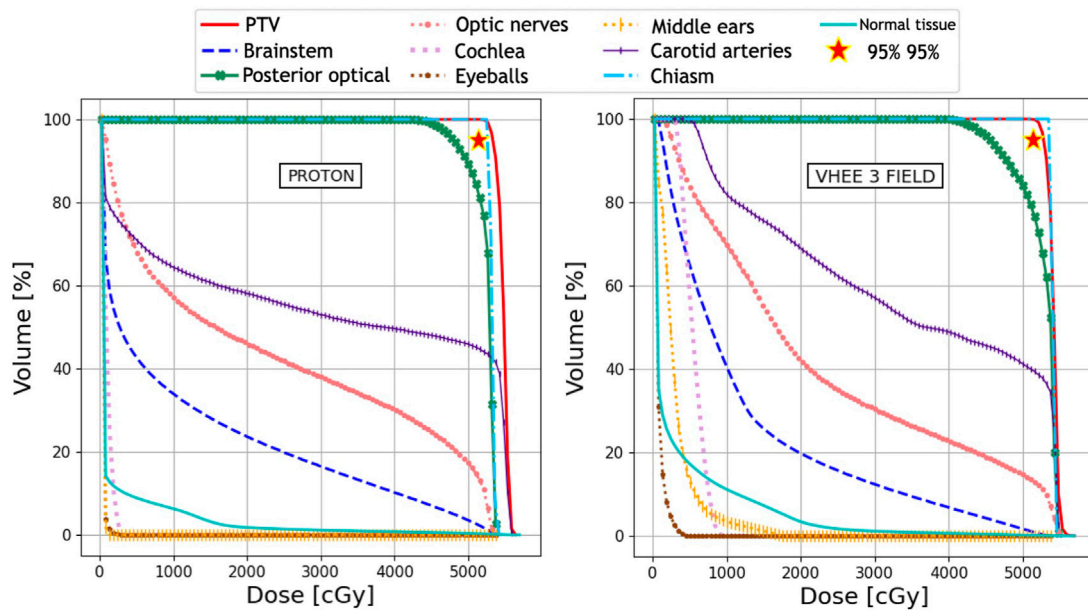
FIGURE 3
Plan comparison between PT and VHEE for patient M1. DVHs for the PTV and OARs from the PT plan are reported on the left, whereas the VHEE results obtained assuming an irradiation with three fields are shown on the right. The absorbed dose relative to the unspecified normal tissue (NoT in the legend) is also shown.

The actual values of D_T and FMF^m that are used in a real case scenario are strongly dependent on the outcome of the ongoing experimental campaign that aims at defining the FLASH conditions in terms of the absorbed dose, dose rate, and

fractionation schemes [10]. Therefore, FMF^m equal to 0.8 was chosen, a value that can be optimistically used at this moment to describe what can be expected as OAR sparing for internal organs during FLASH irradiations. Tissue-dependent values were not

TABLE 4 Values of V_{XX} and D_1 for the PTV and different OARs relevant to the planning of patient M1. Different columns show the values obtained from the proton, IMRT, VHEE with three fields, and VHEE with seven field . The result obtained for the carotid arteries is given in terms of V_{105}. All the obtained values satisfy the requirements shown in Table 1.

M1	Parameter	Proton	Photon	VHEE with three fields	VHEE with seven fields
PTV	$V_{95\%}$	100%	99.30%	98.97%	97.00%
	$V_{105\%}$	0.01%	0.009%	0.05%	1.27%
Optic nerves	D_1	52.98 Gy	53.76 Gy	54 Gy	54 Gy
Chiasm	D_1	53.52 Gy	54 Gy	53.68 Gy	53.71 Gy
Posterior optical path	D_1	53.58 Gy	53.82 Gy	53.94 Gy	53.67 Gy
Eyeballs	D_1	1.25 Gy	10.52 Gy	3.30 Gy	11.82 Gy
Brainstem	D_1	52.59 Gy	51.99 Gy	50.40 Gy	51.02 Gy
Carotid arteries	$V_{105\%}$	0.03%	9.11%	2.54%	1.16%

FIGURE 4
Plan comparison between IMRT and VHEE for patient C1. DVHs for the PTV and OARs from the IMRT plan are reported on the left, whereas the VHEE results obtained assuming an irradiation with seven fields are shown on the right. The absorbed dose relative to the unspecified normal tissue (NoT in the legend) is also shown.
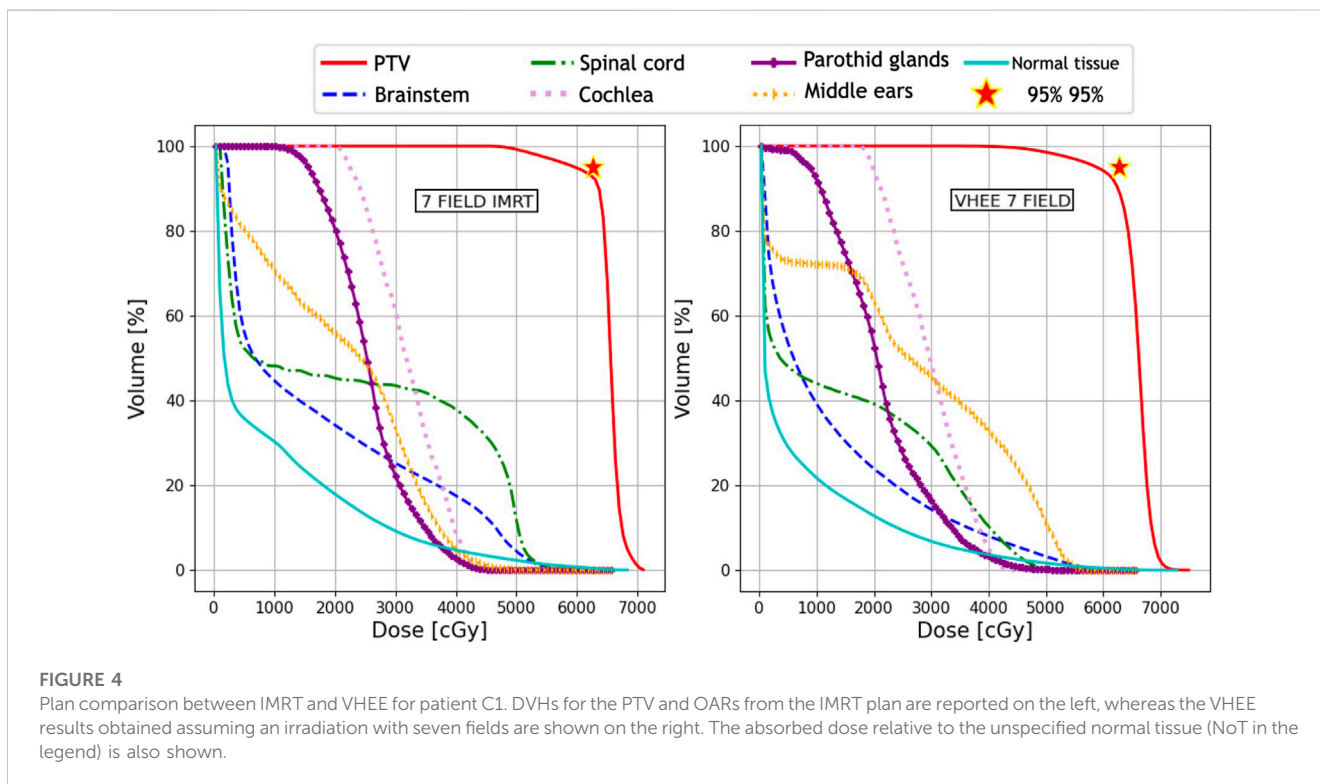
implemented, and the same FMF value (computed accordingly to Eq. 1) was used for all the voxels that did not belong to the PTV and are either described as OARs or normal tissue (NoT).

The evaluation of the FLASH effect potential was performed after treatment optimisation. Once the final dose maps were available, the dose in each voxel was rescaled by the FMF from Eq. 1, and then the DVH calculation and evaluation of plan adequacy were re-assessed.

3 Results

The absorbed dose maps for the three techniques (IMRT, PT, and VHEE) were used to compute the DVHs and quantitatively compare the treatment plans. The DVH comparisons are shown in Figure 2 (IMRT vs. VHEE) and Figure 3 (PT vs. VHEE) for M1 and in Figure 4 (IMRT vs. VHEE) and Figure 5 (PT vs. VHEE) for C1.

For plan comparisons, VHEE plan optimisation was performed assuming the same field number and geometry (same gantry angle) as those adopted with the other radiotherapeutic techniques (see also Section 2.1).

The optimised dose maps for all the patients and radiation types are shown in Supplementary Appendix Figures S8, S9 which show the results, respectively, for M1 and C1 using IMRT, PT, and the different VHEE field geometries. The isodose curves are shown in Supplementary Appendix Figures S11, S12.

Figure 2 demonstrates that IMRT and VHEE plans have a comparable quality: while IMRT provides a better PTV coverage,

FIGURE 5
Plan comparison between PT and VHEE for patient C1. DVHs for the PTV and OARs from the PT plan are reported on the left, whereas the VHEE results obtained assuming an irradiation with four fields are shown on the right. The absorbed dose relative to the unspecified normal tissue (NoT in the legend) is also shown.
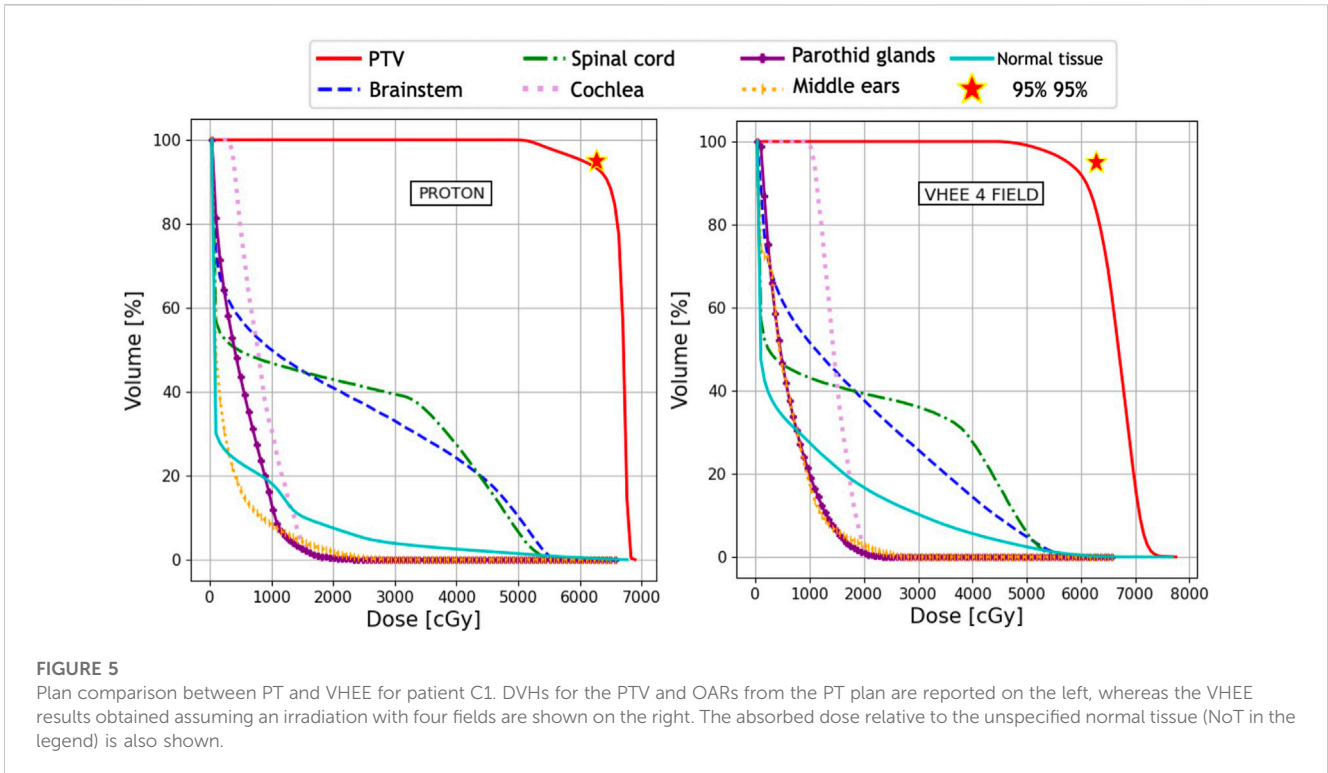
TABLE 5 Values of V_{XX}, D_{mean}, and D_1 for the PTV and different OARs relevant for the planning of patient C1. Different columns show the values obtained from the proton, IMRT, VHEE with four fields, and VHEE with seven fields plans. All the obtained values satisfy the requirements shown in **Table 2**.

C1	Constraint	Proton	Photon	VHEE with four fields	VHEE with seven fields
PTV boost	$V_{95\%}$	93.57%	92.96%	85.52%	90.61%
	$V_{105\%}$	0%	3.05%	28.32%	6.12%
Brainstem	D_1	54.64 Gy	53.79 Gy	55.04 Gy	55.15 Gy
Spinal cord	D_1	53.39 Gy	54.04 Gy	53.54 Gy	47.77 Gy
Parotid glands	D_{mean}	4.74 Gy	25.29 Gy	5.73 Gy	20.82 Gy
Middle ears	D_{mean}	2.63 Gy	20.63 Gy	5.40 Gy	25.94 Gy
Cochlea	D_{mean}	7.98 Gy	31.54 Gy	14.32 Gy	29.39 Gy

the VHEE irradiation is better at sparing the cochlea. In addition, Figure 3 shows that the VHEE configuration with three fields provides a better PTV coverage than the configurations with seven fields, matching the performance of the PT plan. A quantitative analysis supporting these statements is shown in Table 4, where the values of interest for evaluating the plan goodness are shown for all the M1 treatment plans.

C1 is a more complex case where OAR sparing limits the PTV coverage for all plans. For this reason, priority was given to limit the absorbed dose to the brainstem and spinal cord even if this meant not reaching the desired PTV coverage. For this patient, the DVH analysis of the VHEE configurations with four and seven fields, as shown in Figure 4 and Figure 5, indicates that increasing the number of fields can help in improving the target coverage: the PTV boost

coverage shown in the first row in terms of $V_{95\%}$ increases from 85.5% to 90.6%.

The values of V_{XX}, D_{mean}, and D_1 that are used to evaluate the C1 plan are shown in Table 5. Although VHEEs achieve a lower coverage of the PTV, they also result in a better sparing of the spinal cord. The comparison between the irradiation with four and seven fields clearly shows that different geometries can be explored to provide a better sparing of given OARs, and as an example, it is possible to observe that the ear canals, the cochlea, and the parotid glands receive a significantly different mean dose in the two cases.In summary it is possible to conclude that all plans obtained with PT, IMRT, and VHEE, both for M1 and C1, satisfy the constraints and are compatible with the clinical prescriptions.
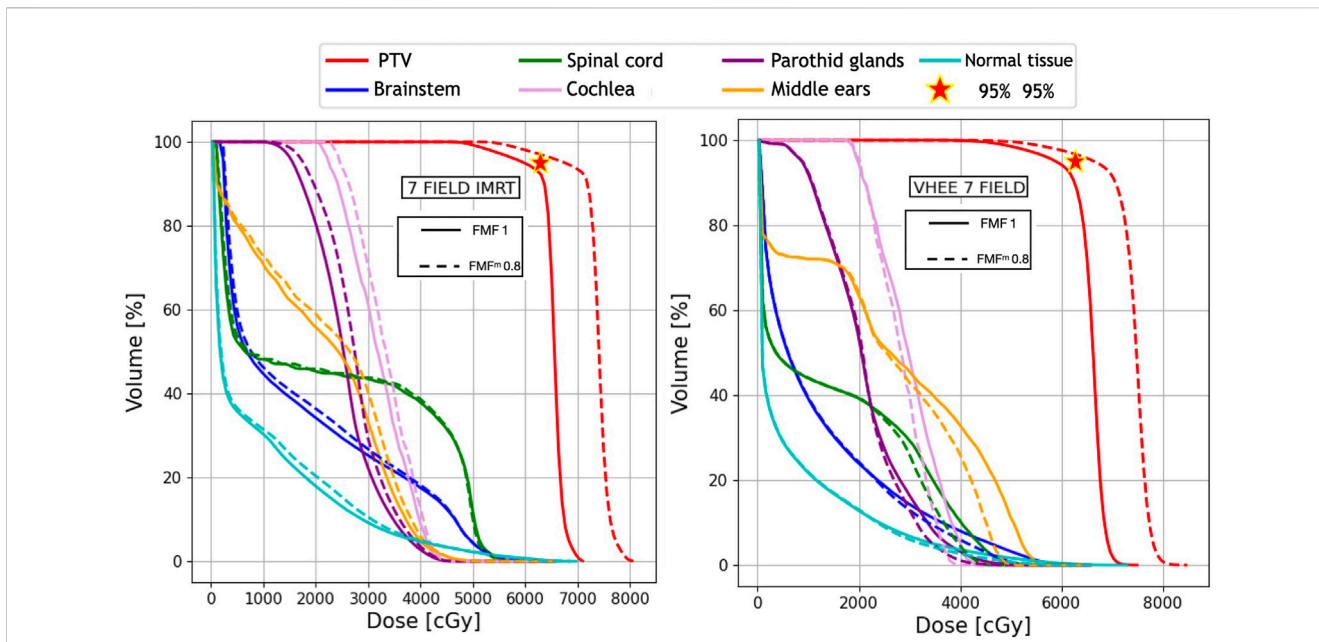
FIGURE 6
Plan comparison between IMRT and VHEE for patient C1. The biological dose relative to an FMF^m of 0.8 is shown in dashed lines. DVHs for the PTV, OARs, and NoT from the IMRT plan are reported on the left, whereas the VHEE results obtained assuming an irradiation with seven fields (see Table 3) are shown on the right.
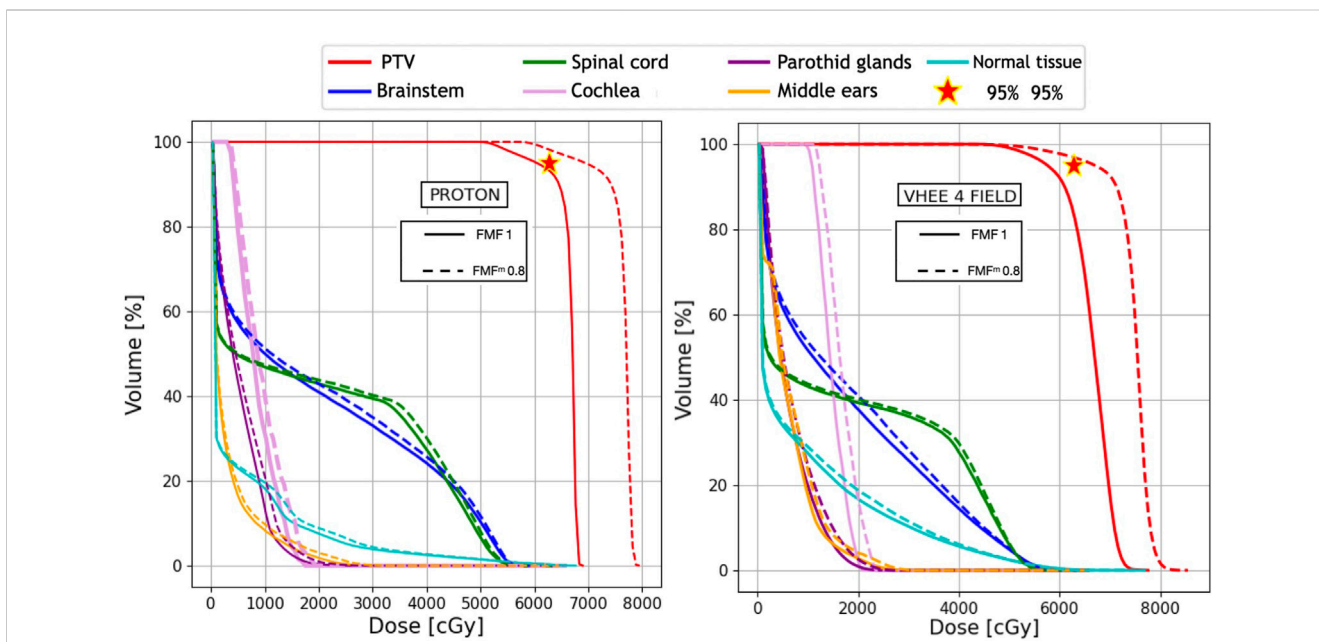
FIGURE 7
Plan comparison between PT and VHEE for patient C1. The biological dose relative to an FMF^m of 0.8 is shown in dashed lines. DVHs for the PTV, OARs, and NoT from the PT plan are reported on the left, whereas the VHEE results obtained assuming an irradiation with four fields (see Table 3) are shown on the right.

3.1 FLASH effect impact

The optimised plans have also been used to evaluate the potential of FLASH irradiation. Thus, the absorbed dose maps for each plan have been processed, and the absorbed dose in each voxel not belonging to the PTV has been multiplied by the FMF(D) value computed according to Eq. 1. In this way, the sparing of the OARs due to the FLASH effect was accounted for and DVHs

TABLE 6 Values of V$_{XX}$, D$_{mean}$, and D$_1$ obtained after considering the reduced biological dose due to FMF(D) sparing of patient M1. V$_{105\%}$ relative to the carotid arteries becomes negligible and it is not shown.

M1	Constraint	Proton	IMRT	VHEE with three fields	VHEE with seven field
PTV	$V_{95\%}$	100%	99.30%	98.97%	97.00%
	$V_{105\%}$	0.01%	0.009%	0.05%	1.27%
Optic nerves	D_1 Gy(FMF)	46.39	47.51	47.64	47.29
Chiasm	D_1 Gy(FMF)	47.47	46.81	47.38	47.36
Posterior optical path	D_1 Gy(FMF)	46.86	47.47	47.59	47.26
Eyeballs	D_1 Gy(FMF)	1.25	9.73	3.34	11.98
Brainstem	D_1 Gy(FMF)	46.07	45.94	44.74	43.77

TABLE 7 Values of V$_{XX}$, D$_{mean}$, and D$_1$ obtained after considering the reduced biological dose due to FMF(D) sparing of patient C1, and an overall absorbed dose scaling is applied to increase the PTV coverage while maintaining the dose inside the OARs under an affordable limit.

C1	Constraint	PROTON	IMRT	VHEE with four fields	VHEE with seven fields
PTV boost	$V_{95\%}$	97.71%	96.65%	96.58%	96.43%
	$V_{105\%}$	95.27%	92.84%	91.04%	93.08%
Brainstem	D_1 Gy(FMF)	54.85	54.79	54.76	54.37
Spinal cord	D_1 Gy(FMF)	53.69	53.41	53.39	47.70
Parotid glands	D_{mean} Gy(FMF)	5.44	27.23	6.53	22.67
Middle ears	D_{mean} Gy(FMF)	3.02	21.86	6.14	26.69
Cochlea	D_{mean} Gy(FMF)	9.06	33.02	16.33	31.07

were re-evaluated. The impact of the FLASH effect on sparing the OARs, according to the assumptions made here previoulsy, can be observed in DVHs shown in Figure 6 and Figure 7.

Table 6 shows the results obtained for patient M1. In this case, as the PTV coverage is already satisfactory without invoking the FLASH effect, the latter would produce an additional reduction of the dose absorbed by OARs and therefore resulting in additional OAR sparing. When compared to Table 4, it is possible to observe the significant reduction in D_1, from 55 to 47 Gy(RBE), for the OARs that are located close to the PTV. DVHs are computed by taking into account FLASH sparing, as shown in the Appendix, in Supplementary Appendix Figure S10.

For C1, where the PTV coverage is limited by the dose constraints on the OARs, a different approach was followed: the D_1 values were computed once the FLASH effect was applied, and then the overall dose was rescaled until the limit on OAR sparing (54 Gy) was reached. Under that condition, the PTV coverage was assessed to determine the net increase that could be achieved by exploiting the FLASH effect. The results are shown in Figure 6 and Figure 7, respectively, for IMRT compared with VHEE using seven irradiation fields and PT compared with VHEE using four irradiation fields.

The results obtained for patient C1 are shown in Table 7, demonstrating that the additional OAR sparing provided by the FLASH effect could be exploited to increase the PTV coverage when

treating such lesions. Profiting from the reduced absorbed dose, it was possible to reach a PTV coverage with $V_{95\%}$ larger than 95% while satisfying the dose limits on the brainstem. The irradiation using seven fields, in this case, provides a PTV coverage comparable with the irradiation achievable with four fields but, in addition, allows for better sparing of the spinal cord.

4 Discussion

The potential of VHEE irradiations of intracranial lesions using a small number (between three and seven) of mono-energetic fields and assuming an active-scanning-like beam delivery strategy has been explored.

VHEE with maximum energy of 130 MeV were found to be suitable for the treatment of deep-seated tumours in disease sites with difficult irradiation geometries, allowing a limited number of fields to achieve performances comparable with PT and IMRT. This result, obtained under the assumption of a conventional dose rate, is promising in itself, as it suggests that compact electron accelerators could provide appropriate treatment quality at an affordable cost and with minimal impact on the infrastructures [25], thus providing a valid alternative to PT and IMRT treatments.

The VHEE plans obtained with different irradiation geometries demonstrated that there is a significant room for improvement when

trying to optimise not only the beam fluence to cover the target volume but also the field geometry and its energy. The lack of experience in planning treatments with electrons makes it hard to assess if the best possible configurations are the configurations already tested in this manuscript, without an automated tool that can systematically explore the different number of fields, irradiation directions, and beam energies like what is currently performed for photons and protons. The full potential of VHEE will be reassessed once such tool will finally be available.

The beam scanning method used for VHEE treatments allowed us to reach the desired absorbed dose conformity to the PTV while maintaining each field mono-energetic. This condition plays a crucial role when discussing the suitability of VHEE to be used for FLASH therapy irradiations; since there is no need to change the energy within a field, each field can be delivered in a very short time (no more than a few hundred ms), making it easier to achieve an Ultra-High Dose Rate (UHDR) regime. The technological challenge of delivering more than one field in a very short period of time required to ensure FLASH sparing of the OARs is to be addressed yet, but one thing that VHEE plans have in common with proton plans is especially the number of fields that have to be delivered is, in some cases, identical (e.g., the case of M1).

The potential impact of FLASH in terms of OAR sparing has been explored as well, under reasonable assumptions that a maximum sparing effect between 20% and 35% could be achieved, whenever the total absorbed dose in each voxel exceeded the 20 Gy threshold. Meanwhile, although the values of FMF^m and D_T still need an extensive experimental characterisation and have been assumed to be constant against different types of tissues and independent of the dose rate, the results show that the additional sparing obtained from UHDR would be helpful in improving OAR sparing (e.g., in the case of M1) or allowing for dose escalation that could be used to improve the PTV coverage (as in the case of C1). In both cases, the FLASH effect could be exploited to improve the treatment efficacy, broadening the therapeutic window of the treatment. Both pancreatic cancer and lung cancer seem to be particularly interesting in this respect: hypo-fractionation regimes have already been explored for such treatments, thus representing good candidates to account for the dose and dose rate dependencies of the FMF in a realistic clinical scenario.

The rather basic handling of FLASH effect modelling implemented in this study follows the limited experimental knowledge of the conditions needed to trigger OAR sparing. In this work, no dependence of the FMF on the tissue type or the dose rate was considered. The comparison of the results obtained with FMF equal to 1 (no FLASH effect) and implementing an FMF that has a dose-dependence based on real data with an asymptotic value of 0.8 allow for evaluating the FLASH potential under a robust, well-defined condition that reflects the current best experimental description of the effect. As no fractionation scheme compatible with UHDR irradiations is currently available, for the irradiation of intracranial lesions, we have also decided to maintain the plan constraints coming from the conventional fractionation scheme (2 Gy per fraction). The results presented are not aiming at evaluating which plan, among RT, PT, and VHEE, is the best for the treatment of the specific intracranial lesions used for the simulation study. Instead the main purpose of the presented study is to allow a robust and fair evaluation of the VHEE potential both in conventional and UHDR irradiation modalities.

A refined experimental input, and a better modelling of the FMF, when available, will be used to improve the evaluations presented in this contribution, allowing for a better estimate of the FLASH therapy advantages achievable in a clinical scenario.

5 Conclusion

The treatment of intracranial lesions with VHEE has been explored. VHEEs were compared against IMRT and PT plans for two patients previously treated with protons, and the results demonstrated that VHEE can achieve performances that are comparable with the state-of-the-art irradiation techniques even in the absence of additional sparing provided by the FLASH effect.

Considering that the VHEE mono-energetic beam interaction with the patient's tissue results in an absorbed dose distribution that exhibits a very broad peak, and that FLASH rates have already been demonstrated to be deliverable for low-energy electron applications (IOeRT [26, 27]), it was also possible to explore the additional increase that could be achieved when switching to a UHDR configuration. The results demonstrate that under reasonable assumptions on the conditions needed to trigger the FLASH effect, and on its actual value, the FLASH effect could effectively be used to reduce the impact on the OARs surrounding the PTV or to improve the PTV coverage, depending on the actual characteristics of the target volume and the constraints on the OARs crossed by the beam. In all cases and for all particle types, the FLASH effect showed a clear potential in significantly improving the therapeutic window of EBRT treatments.

Data availability statement

The raw data supporting the conclusions of this article will be made available by the authors, without undue reservation.

Ethics statement

Ethical review and approval was not required for the study on human participants, and written informed consent for participation was obtained.

Author contributions

ASar, AM, AdG, MS, GF, MP, ASch, and VP wrote the main manuscript text. ASar, MS, GF, MM, and ASch prepared the figures. LC, DC, FdF, CdF, MP, MS, SS, and VT provided information about the dosimetric constraints that plans have to satisfy and the treatment plans with photons and protons. GB, YD, IM, RM, LP, SM, and MT defined the dose-modifying factor modelling inside the optimisation algorithms. LP, ASch, ASci, and ASar provided information about the beam model to be used in the Monte Carlo simulations. LA, MdS, IM, RM, SM, VP, LR, DR, ASar, ASch, GT, MT, and AT implemented the simulation, optimization algorithms, and performed the data analysis. All

authors contributed to the article and approved the submitted version.

Conflict of interest

ASa and VPa participated in research projects funded by the company Sordina IORT Technologies (SIT). The research was also funded by the royalties of the TPS system developed for the SIT IOeRT machine.

The remaining authors declare that the research was conducted in the absence of any commercial or financial relationships that could be construed as a potential conflict of interest.

The reviewer OS declared a past co-authorship with the authors MDS to the handling Editor.

Publisher's note

All claims expressed in this article are solely those of the authors and do not necessarily represent those of their affiliated organizations, or those of the publisher, the editors, and the reviewers. Any product that may be evaluated in this article, or claim that may be made by its manufacturer, is not guaranteed or endorsed by the publisher.

Supplementary material

The Supplementary Material for this article can be found online at: https://www.frontiersin.org/articles/10.3389/fphy.2023.1185598/full#supplementary-material

References

1. Bazalova-Carter M, Qu B, Palma B, Hårdemark B, Hynning E, Jensen C, et al. Treatment planning for radiotherapy with very high-energy electron beams and comparison of vhee and vmat plans. *Med Phys* (2015) 42:2615–25. doi:10.1118/1.4918923

2. Schüler E, Eriksson K, Hynning E, Hancock SL, Hiniker SM, Bazalova-Carter M, et al. Very high-energy electron (vhee) beams in radiation therapy; treatment plan comparison between vhee, vmat, and ppbs. *Med Phys* (2017) 44:2544–55. doi:10.1002/mp.12233

3. Krim D, Rrhioua A, Zerfaoui M, Bakari D. Monte Carlo modeling of focused very high energy electron beams as an innovative modality for radiotherapy application. *Nucl Instr Methods Phys Res Section A: Acc Spectrometers, Detectors Associated Equipment* (2023) 1047:167785. doi:10.1016/j.nima.2022.167785

4. Ronga MG, Cavallone M, Patriarca A, Leite AM, Loap P, Favaudon V, et al. Back to the future: Very high-energy electrons (vhees) and their potential application in radiation therapy. *Cancers* (2021) 13. doi:10.3390/cancers13194942

5. Maxim PG, Tantawi SG, Loo BW. Phaser: A platform for clinical translation of flash cancer radiotherapy. *Radiother Oncol* (2019) 139, 28–33. FLASH radiotherapy International Workshop. doi:10.1016/j.radonc.2019.05.005

6. Giuliano L, Bosco F, Carillo M, Arcangelis D, Ficcadenti L, Migliorati M, et al. *Preliminary studies of a compact vhee linear accelerator system for flash radiotherapy* (2021). doi:10.18429/JACoW-IPAC2021-MOPAB410

7. Venkatesulu BP, Sharma A, Pollard-Larkin JM, Sadagopan R, Symons J, Neri S, et al. Author correction: Ultra high dose rate (35 gy/sec) radiation does not spare the normal tissue in cardiac and splenic models of lymphopenia and gastrointestinal syndrome. *Scientific Rep* (2020) 10:1. doi:10.1038/s41598-020-67913-7

8. Bourhis J, Montay-Gruel P, Gonçalves Jorge P, Bailat C, Petit B, Ollivier J, et al. Clinical translation of flash radiotherapy: Why and how? *Radiother Oncol* (2019) 139, 11–7. FLASH radiotherapy International Workshop. doi:10.1016/j.radonc.2019.04.008

9. Bourhis J, Sozzi WJ, Jorge PG, Gaide O, Bailat C, Duclos F, et al. Treatment of a first patient with flash-radiotherapy. *Radiother Oncol* (2019) 139, 18–22. FLASH radiotherapy International Workshop. doi:10.1016/j.radonc.2019.06.019

10. Vozenin MC, Bourhis J, Durante M. Towards clinical translation of flash radiotherapy. *Nat Rev Clin Oncol* (2022) 19:791–803. Cited By 2. doi:10.1038/s41571-022-00697-z

11. Montay-Gruel P, Corde S, Laissue JA, Bazalova-Carter M. Flash radiotherapy with photon beams. *Med Phys* (2022) 49:2055–67. doi:10.1002/mp.15222

12. Zhang G, Zhang Z, Gao W, Quan H. Treatment planning consideration for very high-energy electron flash radiotherapy. *Physica Med* (2023) 107:102539. doi:10.1016/j.ejmp.2023.102539

13. Sarti A, De Maria P, Battistoni G, De Simoni M, Di Felice C, Dong Y, et al. Deep seated tumour treatments with electrons of high energy delivered at flash rates: The example of prostate cancer. *Front Oncol* (2021) 11. doi:10.3389/fonc.2021.777852

14. Narayanasamy G, Saenz D, Cruz W, Ha CS, Papanikolaou N, Stathakis S. Commissioning an elekta versa hd linear accelerator. *J Appl Clin Med Phys* (2016) 17:179–91. doi:10.1120/jacmp.v17i1.5799

15. Xia P, Murray E. 3d treatment planning system—Pinnacle system. *Med Dosimetry* (2018) 43:118–28. Special Issue: 3D Treatment Planning Systems. doi:10.1016/j.meddos.2018.02.004

16. Rahman M, Trigilio A, Franciosini G, Moeckli R, Zhang R, Böhlen TT. Flash radiotherapy treatment planning and models for electron beams. *Radiother Oncol* (2022) 175:210–21. doi:10.1016/j.radonc.2022.08.009

17. Poppinga D, Kranzer R, Farabolini W, Gilardi A, Corsini R, Wyrwoll V, et al. Vhee beam dosimetry at cern linear electron accelerator for research under ultra-high dose rate conditions. *Biomed Phys Eng Express* (2020) 7:015012. doi:10.1088/2057-1976/abcae5

18. Labate L, Palla D, Panetta D, Avella F, Baffigi F, Brandi F, et al. Toward an effective use of laser-driven very high energy electrons for radiotherapy: Feasibility assessment of multi-field and intensity modulation irradiation schemes. *Scientific Rep* (2020) 10. doi:10.1038/s41598-020-74256-w

19. Ferrari A, Sala PR, Fasso A, Ranft J. *Fluka: A multi-particle transport code (program version 2005)* (2005). CERN-2005-010, SLAC-R-773, INFN-TC-05-11.

20. Battistoni G, Bauer J, Boehlen TT, Cerutti F, Chin MPW, Dos Santos Augusto R, et al. The fluka code: An accurate simulation tool for particle therapy. *Front Oncol* (2016) 6:116. doi:10.3389/fonc.2016.00116

21. Schaffner B, Pedroni E, Lomax A. Dose calculation models for proton treatment planning using a dynamic beam delivery system: An attempt to include density heterogeneity effects in the analytical dose calculation. *Phys Med Biol* (1999) 44:27–41. doi:10.1088/0031-9155/44/1/004

22. Wilson JD, Hammond EM, Higgins GS, Petersson K. Ultra-high dose rate (flash) radiotherapy: Silver bullet or fool's gold? *Front Oncol* (2020) 9:1563. doi:10.3389/fonc.2019.01563

23. Wilson JD, Hammond EM, Higgins GS, Corrigendum PK. Ultra-high dose rate (flash) radiotherapy: Silver bullet or fool's gold? *Front Oncol* (2020) 10:210. doi:10.3389/fonc.2020.00210

24. Bohlen TT, Germond JF, Bourhis J, Vozenin MC, Ozsahin EM, Bochud F, et al. Normal tissue sparing by flash as a function of single-fraction dose: A quantitative analysis. *Int J Radiat Oncol Biol Phys* (2022) 114:1032–44. A Red Journal Special IssueOligometastasis, Part 2. doi:10.1016/j.ijrobp.2022.05.038

25. Faillace L, Alesini D, Bisogni G, Bosco F, Carillo M, Cirrone P, et al. Perspectives in linear accelerator for flash vhee: Study of a compact c-band system. *Physica Med* (2022) 104:149–59. doi:10.1016/j.ejmp.2022.10.018

26. Felici G, Barca P, Barone S, Bortoli E, Borgheresi R, De Stefano S, et al. Transforming an iort linac into a flash research machine: Procedure and dosimetric characterization. *Front Phys* (2020) 8. doi:10.3389/fphy.2020.00374

27. Calvo FA, Serrano J, Cambeiro M, Aristu J, Asencio JM, Rubio I, et al. Intra-operative electron radiation therapy: An update of the evidence collected in 40 years to search for models for electron-flash studies. *Cancers* (2022) 14. doi:10.3390/cancers14153693